Materials Letters 358 (2024) 135883

Contents lists available at ScienceDirect

Materials Letters

journal homepage: www.elsevier.com/locate/matlet

One-pot synthesis of mechanically robust hierarchical graphene-polyethylene aerogels

Amirarsalan Mashhadian [a], Siyu Tian [a], Shiwen Wu [a], Ruda Jian [a], Fateme Najafkhani Feijani [a], Feifei Fan [b], Hongbing Lu [a], Guoping Xiong [a,*]

[a] Department of Mechanical Engineering, The University of Texas at Dallas, 800 W Campbell Rd, Richardson, TX 75080, United States
[b] Department of Mechanical Engineering, University of Nevada, Reno, Reno, NV 89557, United States

ARTICLE INFO

Keywords:
Graphene aerogel
Composite
Mechanical properties
Polymer
Elastic

ABSTRACT

Fabricating mechanically robust graphene aerogels (GAs) without compromising their notable features including superelasticity, large surface area, high porosity, and low density is challenging. This work presents a new one-pot strategy based on ambient drying to fabricate a three-dimensional (3D) graphene-polyethylene aerogel (G-PEA) with a unique hierarchical porous structure, in which the highly porous polyethylene is encapsulated by graphene frameworks. The hierarchical G-PEA exhibited substantially enhanced compressive strength while maintaining low density and superelasticity comparable to those of bare GAs. The G-PEAs with 5 wt% PE (G-PEA5) showed a significant improvement (up to 2083 %) in compressive stress compared to bare GAs, which can be attributed to the porous PE support within the GA framework. The G-PEA5 retained 94 % of its compressive stress after 100 compression cycles, which is still higher than that (~80 %) of bare GAs, and maintained good elastic recovery. The designed hierarchical G-PEAs show great promise in the applications that require outstanding mechanical properties.

1. Introduction

Three-dimensional (3D) graphene aerogels (GAs) have been utilized in various applications including sensing, medicine, robotics, and energy storage because of their high porosity, large surface area, low mass density, and superelasticity [1–3]. However, the mechanical strength of GAs is relatively low, limiting their functionality in practical applications [4,5]. To combat this issue, several methods have been used such as structural modification of GAs and polymer reinforcement where GA pores were completely filled with polymers [6,7]. Controlling wall thickness, pore size and mass density of GAs could ameliorate the mechanical properties, and yet the mechanical strength needs further improvement [8]. Integrating polymers into the GA framework led to a dense composite, making it less attractive compared to GAs [9]. Therefore, tailoring the structure of the graphene-polymer aerogels is critical to tackle the intrinsic trade-off between strength and other unique features of GAs including elasticity, high porosity, and low density.

In this paper, a new one-pot strategy based on ambient drying is proposed to improve the mechanical properties of GAs while retaining their lightweight, superelasticity, and high porosity. By encapsulating PE into the graphene frameworks via emulsification, lightweight graphene-polyethylene aerogels (G-PEAs) with unique hierarchical structures and outstanding mechanical properties was obtained. With porous PE filling the large GA pores, the graphene network will be prevented from fracture under high compressive strains. Compared to bare GAs, the G-PEA with 5 wt% PE (G-PEA5) composite showed a considerable enhancement of compressive strength up to 2083 % with improved deformation recovery and comparable compressibility over 100 cycles. This work offers a new strategy for the scalable manufacturing of high-performance graphene-based aerogels.

2. Experimental methods

2.1. Preparation of the aerogels

Graphene oxide (GO) was synthesized following the procedures described in our prior work [10]. Different amounts of PE (1.5, 0.75, 0 g) with a mass density of 27 mg/cm^3 were dissolved in camphene (13.5 g) at 90 °C. Then, 15 g of prepared GO (25 mg/mL) was added to the PE/

* Corresponding author.
E-mail address: Guoping.Xiong@utdallas.edu (G. Xiong).

https://doi.org/10.1016/j.matlet.2024.135883
Received 7 September 2023; Received in revised form 9 December 2023; Accepted 2 January 2024
Available online 3 January 2024

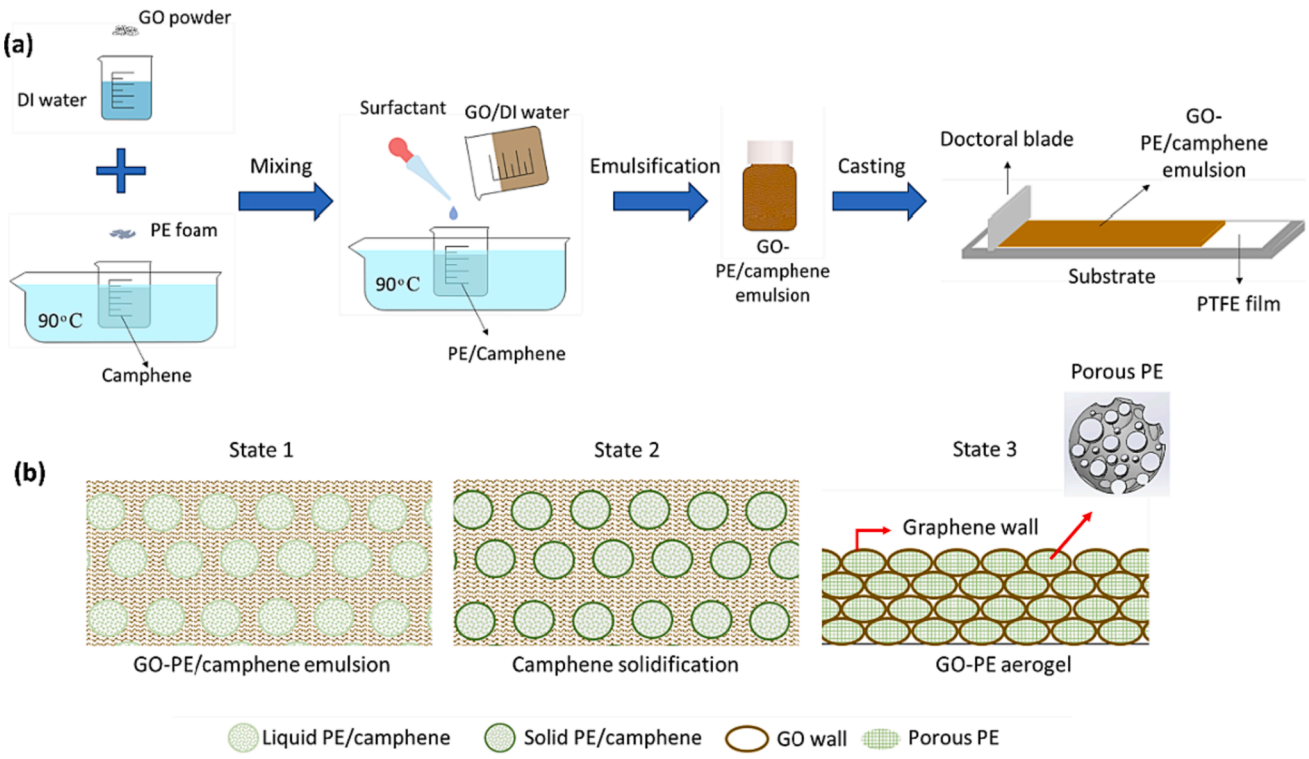

Fig. 1. Schematics showing the fabrication procedures: (a) schematic of the fabrication process of porous GO-PE composite, (b) schematic of GO-PE/camphene emulsion (state 1), camphene solidification (state 2) and GO-PE aerogel (state 3).

camphene mixture. Sodium dodecyl sulfate (0.375 mL, 250 mg/mL) was added to the mixture, followed by mechanical shaking to form a homogeneous emulsion. The obtained emulsions were cast on Teflon films with a height of 5 mm using a doctoral blade. The cast emulsions were dried for 3 days at ambient condition (24 °C, 1 atm) to obtain GO-PE aerogels with a final height of 1.40 mm. The hierarchical G-PEA was obtained through hydrazine reduction in a sealed container kept at 40 °C for 18 h [11]. The prepared G-PEA composites with 0 wt%, 2.5 wt% and 5 wt% are denoted as G-PEA0, G-PEA2.5, and G-PEA5, respectively. Finally, G-PEA composites were cut into desired shapes using a laser cutter (VLS3.60DT, ULS) for testing.

2.2. Characterization

The emulsion drying process was imaged by an optical microscope (OM, AmScope B120). After drying process, the morphologies of the obtained composites were characterized by a field-emission scanning electron microscope (SEM, Zeiss supra 40). Thermogravimetric analysis

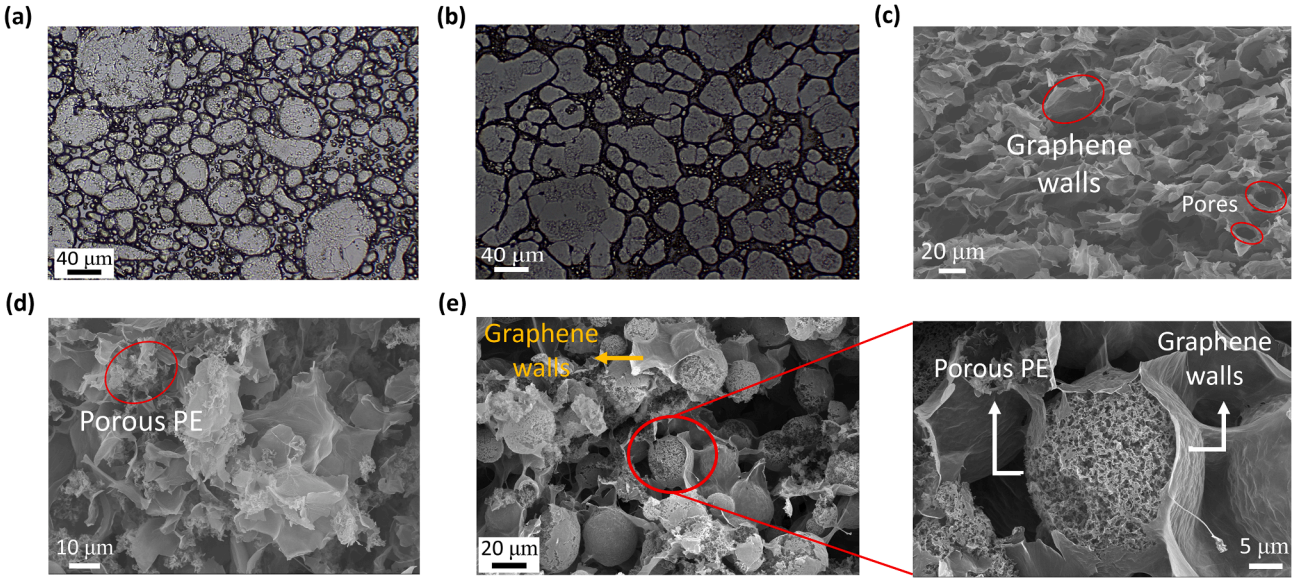

Fig. 2. Optical images of the GO-PE/camphene at different solidification states with a GO concentration of 25 mg/mL: (a) Liquid PE/camphene encapsulated by GO solution (state 1). (b) Solidified PE/camphene encapsulated by GO solution (state 2). SEM images of GAs with different PE concentrations (state 3): (c) G-PEA0, (d) G-PEA2.5, and (e) G-PEA5.

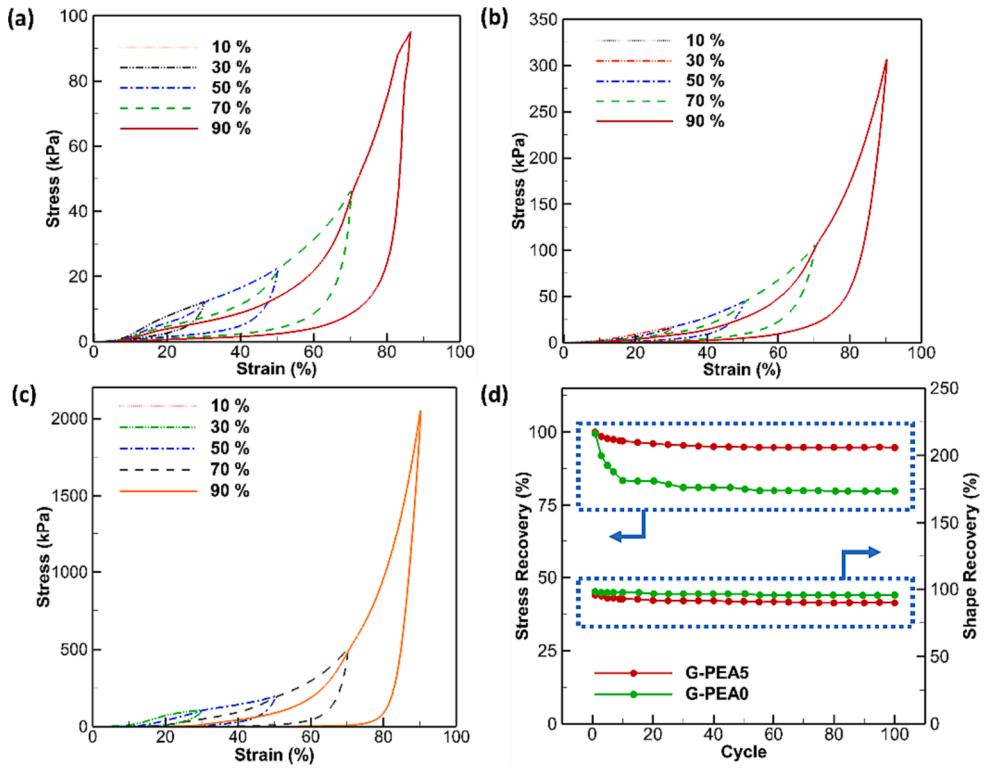

Fig. 3. Compressive mechanical properties of G-PEA composites with a GO concentration of 25 mg/mL. Compressive engineering stress–strain curves of (a) G-PEA0, (b) G-PEA2.5, and (c) G-PEA5. (d) Comparative stress and shape recovery stability of G-PEA0 and G-PEA5 over 100 cycles.

(TGA, TA Instruments) of samples was carried out from 20 to 700 °C with a heating ramp of 10 °C/min under air flow. Brunauer-Emmett-Teller (BET, ASAP 2020 Plus) surface area of G-PEA composites was measured via nitrogen physisorption. Fourier transform infrared (FTIR) was conducted by using an Agilent Carry 660 FTIR spectrophotometer. Mechanical testing was conducted on a universal material testing system (Instron 5567).

3. Results and discussion

Fig. 1a and b schematically show the fabrication procedures of the emulsion and the subsequent drying process of the GO-PE aerogel, respectively. Camphene possesses a melting point of ~50 °C. Consequently, the liquid PE/camphene encapsulated by GO (state 1) rapidly solidifies at ambient temperature (state 2). Upon the sublimation of camphene, porous PE is formed within the GO aerogel pores, resulting in a hierarchical GO-PE aerogel (state 3). The fabricated composites exhibit low densities of 10.93, 24.78, and 60.57 mg/cm^3 for G-PEA0, G-PEA2.5, and G-PEA5, respectively. The fabricated composites represent a high porosity which are comparable with the bare GA (see Table S1).

Fig. 2a illustrates the dissolved PE in camphene in a liquid phase which is encapsulated by GO solution. The subsequent solidification of camphene is shown in Fig. 2b, in which PE/camphene crystals are encapsulated by GO solution. The SEM images in Fig. 2c–e depict the morphologies of the hierarchical aerogels with different PE concentrations. The pore size ranges from 14 to 60 μm in the graphene framework in G-PEA0 (Fig. 2c). Fig. 2d shows the microstructure of G-PEA2.5, in which porous PE was not completely incorporated in GA pores due to the insufficient amount of PE. Fig. 2e exhibits the well-distributed porous PE (pore dimension < 500 nm) encapsulated by graphene sheets, forming a unique hierarchical porous structure of G-PEA5 aerogels. The presence of PE inside the G-PEA2.5 and G-PEA5 samples was further confirmed by FTIR results (Fig. S1). However, adding PE with concentrations higher than 5 wt% to the GA framework led to poor elasticity of the composite. Thermal stability of G-PEA5 was superior to that of G-PEA2.5 and G-PEA0 (Fig. S2), which might be attributed to the strong PE and GA interactions forming a thermally more stable composite [12].

Compression testing was conducted to determine the influence of PE concentrations on the mechanical properties of the composite aerogels. Fig. 3a depicts the compressive stress versus compressive strain for G-PEA0 with the highest obtained compressive stress of 93.98 kPa at 90 % strain. The maximum compressive stress of G-PEA2.5 increased to 306.55 kPa (Fig. 3b) due to the partial formation of the hierarchical structure. As shown in Fig. 3c, the compressive stress of G-PEA5 increased to 2052.03 kPa because of the porous PE encapsulated in the GA frameworks. The G-PEA5 exhibited remarkable height recovery when subjected to 90 % compression strain, as depicted in Fig. S3 and Video S1. The compressive stress of G-PEA5 is significantly enhanced compared to G-PEA0 (i.e., bare GA) and outperforming previously reported GA composites with robust mechanical properties, including high compressive stress and elasticity (see Table S2) [4,6,13,14]. Ambient-dried G-PEAs exhibited superior mechanical properties than those of freeze-dried aerogels due to the suppression of graphene sheets collapse (Fig. S4). To discern the influence of PE on the stability of GAs, cyclic compression tests for G-PEA5 and G-PEA0 were carried out. The stress recovery of G-PEA5 was measured to be (94.66 %) over 100 cycles, which is noticeably higher than that (79.8 %) of bare GAs (Fig. 3d). Fig. 3d also displays the height recovery (89.74 %) of G-PEA5, which is comparable to that (95.59 %) of G-PEA0. The height recovery of the G-PEA.

4. Conclusion

A new one-pot strategy is implemented to fabricate G-PEA aerogels with a unique hierarchical porous structure. The G-PEAs are designed to achieve excellent mechanical properties, lightweight, high porosity, and high elasticity simultaneously. The incorporation of porous PE not only contributes to the relatively low density of the prepared aerogel but also

preserves the porous structure of GAs, which is beneficial for applications such as sound transmission loss and thermal insulation. The obtained hierarchical porous structure of the aerogels results in a remarkable improvement (over 20 times) in compressive strength compared to bare GAs. The facile and scalable manufacturing of composite aerogels provide a new strategy to fabricate lightweight, mechanically robust engineering materials for practical energy applications.

CRediT authorship contribution statement

Amirarsalan Mashhadian: Conceptualization, Data curation, Formal analysis, Investigation, Methodology, Validation, Writing – original draft. **Siyu Tian:** Conceptualization, Validation, Writing – review & editing. **Shiwen Wu:** Investigation, Validation, Writing – review & editing. **Ruda Jian:** Formal analysis. **Fateme Najafkhani Feijani:** Investigation. **Feifei Fan:** Funding acquisition, Writing – review & editing. **Hongbing Lu:** Funding acquisition, Writing – review & editing. **Guoping Xiong:** Conceptualization, Funding acquisition, Supervision, Writing – review & editing.

Declaration of competing interest

The authors declare that they have no known competing financial interests or personal relationships that could have appeared to influence the work reported in this paper.

Data availability

Data will be made available on request.

Acknowledgements

G.X. thanks the University of Texas at Dallas startup fund. G.X. and F. F. thank the support of NSF CMMI-1923033. F.N.F. and H.L. acknowledge the support of NSF CMMI-2219347, DoE DE-NA0003962 & DE-NA-0003525, and the Louis A. Beecherl Jr. Chair.

Appendix A. Supplementary data

Supplementary data to this article can be found online at https://doi.org/10.1016/j.matlet.2024.135883.

References

[1] J. Zhang, et al., Sci. Rep. 7 (1) (2017) 4886.
[2] M. Sakhakarmy, S. Tian, L. Raymond, G. Xiong, J. Chen, Y. Jin, Int. J. Adv. Manuf. Technol. 114 (2021) 343–355.
[3] C. Li, et al., Adv. Funct. Mater. 28 (8) (2018) 1704674.
[4] Y. Wu, et al., Nat. Commun. 6 (1) (2015) 6141.
[5] Y. Xia, C. Gao, W. Gao, J. Polym. Sci. 60 (15) (2022) 2239–2261.
[6] H. Hu, Z. Zhao, W. Wan, Y. Gogotsi, J. Qiu, ACS Appl. Mater. Interfaces 6 (5) (2014) 3242–3249.
[7] Q. Zhang, X. Xu, H. Li, G. Xiong, H. Hu, T.S. Fisher, Carbon 93 (2015) 659–670.
[8] H.L. Gao, et al., Nat. Commun. 7 (1) (2016) 12920.
[9] P. Wang, H. Chong, J. Zhang, H. Lu, ACS Appl. Mater. Interfaces 9 (26) (2017) 22006–22017.
[10] S. Tian, et al., Mater. Lett. 328 (2022) 133128.
[11] H.A. Becerril, J. Mao, Z. Liu, R.M. Stoltenberg, Z. Bao, Y. Chen, ACS Nano 2 (3) (2008) 463–470.
[12] J. Liang, J. Nie, H. Zhang, X. Guo, S. Yan, M. Han, Polymers 15 (11) (2023) 2485.
[13] J. Zhang, S. Luo, Y. Ma, R. Li, Y. Jin, L. Qiu, Chin. Chem. Lett. 34 (2) (2023) 107363.
[14] A.K. Kasar, S. Tian, G. Xiong, P.L. Menezes, J. Porous Mater. 29 (4) (2022) 1011–1025.